Research Square

Preprints are preliminary reports that have not undergone peer review.
They should not be considered conclusive, used to inform clinical practice,
or referenced by the media as validated information.

Loss of bisecting GlcNAcylation on MCAM of bone marrow stoma determined pro-tumoral niche in MDS/AML

Feng Guan (guanfeng@nwu.edu.cn)
Northwest University https://orcid.org/0000-0002-6251-2592
Jingjing Feng
Northwest University
Yi Wang
Department of Hematology, Provincial People's Hospital
Bingxin Li
Northwest University
Xinwen Yu
Northwest University
Lei Lei
Northwest University
JinPeng Wu
Northwest University
Xin Zhang
Northwest University
Qiushi Chen
BGI-Shenzhen
Yue Zhou
Northwest University
Junjie Gou
Northwest University
Hongjiao Li
Research institute of hematology, College of Life Sciences
Zengqi Tan
Northwest University
Zhijun Dai
Zhejiang University
Xiang Li
Research institute of hematology, College of Life Sciences

Article

Keywords: Bisecting GlcNAc, MCAM, bone marrow stromal cells, MDS clonal cells, Exosomal miR188-5p

Posted Date: June 22nd, 2022

DOI: https://doi.org/10.21203/rs.3.rs-1749849/v1

License: This work is licensed under a Creative Commons Attribution 4.0 International License.
Read Full License

Version of Record: A version of this preprint was published at Leukemia on November 5th, 2022. See the published version at https://doi.org/10.1038/s41375-022-01748-1.

Abstract

Bone marrow (BM) stroma plays key roles in supporting hematopoietic stem cell (HSC) growth. Glycosylation contributes to the interactions between HSC and surrounding microenvironment. We observed that bisecting N-acetylglucosamine (GlcNAc) structures, in BM stromal cells were significantly lower for MDS/AML patients than for healthy subjects. Malignant clonal cells delivered exosomal miR-188-5p to recipient stromal cells, where it suppressed bisecting GlcNAc by targeting MGAT3 gene. Proteomic analysis revealed reduced GlcNAc structures and enhanced expression of MCAM, a marker of BM niche. We characterized MCAM as a bisecting GlcNAc-bearing target protein, and identified Asn 56 as bisecting GlcNAc modification site on MCAM. MCAM on stromal cell surface with reduced bisecting GlcNAc bound strongly to CD13 on myeloid cells, activated responding ERK signaling, and thereby promoted myeloid cell growth. Our findings, taken together, suggest a novel mechanism whereby MDS/AML clonal cells generate a self-permissive niche by modifying glycosylation level of stromal cells.

Introduction

The bone marrow (BM) niche is part of a physiological microenvironment in which hematopoietic stem cells (HSCs) are maintained and respond to regulatory signals under various physiological conditions[1]. It is also the site of occurrence of hematological malignancies[2]. BM niche dysfunction strongly affects development of hematological malignancies, and vice versa. BM stroma plays major roles in regulation of a variety of cellular processes, particularly quiescence, differentiation, proliferation, maturation, and apoptosis of hematopoietic stem cells[3, 4]. Conversely, the BM niche can be remodeled by hematopoietic malignant cells to generate a pro-tumoral niche surrounding[5, 6]. Crosstalk between BM stromal cells and malignant cells is thus strongly involved in disease initiation and progression.

Over half of human proteins are glycoproteins. Glycosylation is the most common post-translational modification of proteins, and specific glycan patterns frequently serve as stem cell markers. One example is expression by embryonic pluripotent stem cells of Lewis X (LeX), a glycan motif associated with cell surface glycoproteins, proteoglycans, and lipids[7]. Pentaspan transmembrane glycoprotein CD133 is a marker of very primitive hematopoietic stem and progenitor cells (HSPCs), and specific glycosylation on CD133 + cells helps control their maintenance, differentiation, homing, and mobilization [8–10]. Numerous types of glycoconjugates have been shown to interfere with neoplastic cell processes or microenvironments of these cells, leading to malignant progression. Inhibition of N-linked glycosylation on CD82, a member of the tetraspanin/ transmembrane-4 superfamily, regulates N-cadherin clustering on cell membranes and promotes homing of acute myeloid leukemia (AML) cells to BM [11]. Human B cells secrete active sialyltransferase ST6GAL1 to modify the hematopoietic microenvironment and suppress production of neutrophils, eosinophils, and basophils [12].

We demonstrated in 2013 that human HS27a (but not HS5) BM stromal cells facilitated engraftment of clonal cells from myelodysplastic syndrome (MDS) patients, a process mediated by highly expressed

melanoma cell adhesion molecule [MCAM]/CD146 [13]. Our follow-up 2015 study using multi-omics techniques showed that HS5 cells, in comparison with HS27a, have higher expression of bisecting N-acetylglucosamine (GlcNAc) (β1,4-linked GlcNAc attached to core β-mannose residue, catalyzed by MGAT3) [14]. Bisecting GlcNAc modification regulates physicochemical properties of numerous cell surface glycoproteins, notably integrins, growth factor receptors, and adhesion molecules. S. Yue's group reported that bisecting GlcNAc on CD82 suppressed metastasis of ovarian cancer by inhibiting integrin signaling pathway[15], and we observed that bisecting GlcNAc on EGFR suppressed malignant breast cancer phenotype via downregulation of EGFR/Erk signaling[16]. Similarly, pro-metastatic functions of small extracellular vesicles from breast cancer cells were inhibited by modification of bisecting GlcNAc on vesicular integrin β1[17]. In view of these previous findings, we hypothesized that bisecting GlcNAc modification of MCAM (a cell surface glycoprotein) modulates its function and thereby affects the BM niche.

Our analyses demonstrated that levels of the enzyme β1,4-mannosyl-glycoprotein 4-β-N-acetylglucosaminyltransferase (MGAT3) and responding bisecting GlcNAc structures on BM stromal cells were significantly lower for MDS/AML patients than for healthy control subjects. We evaluated the underlying mechanism whereby bisecting GlcNAc remodels the BM niche by modulating MCAM on stromal cells, and thereby affects proliferation of MDS/AML clonal cells.

Materials And Methods

Cell lines and cell culture

Myeloid leukemia cell line KG1a, and BM-derived stromal cell lines HS5 and HS27a, were kindly donated by Prof. H. Joachim Deeg (Fred Hutchinson Cancer Research Center; Seattle, WA, USA). SKM-1, a cell line established from MDS progressing to AML, was donated by Prof. Xiao Li (Sixth People's Hospital, Shanghai Jiao Tong University). These cell lines were all cultured in RPMI 1640 medium (Biological Industries; Beit Haemek, Israel) added with 10% FBS (Biological Industries) and 1% penicillin/streptomycin (Beyotime Biotechnology; Haimen, Jiangsu, China) at 37°C in 5% CO_2 atmosphere.

Generation of conditional MGAT3$^{loxP/loxP}$ mice

MGAT3$^{fl/fl}$ transgenic mice were generated using a homologous combination knockout strategy, in which exon 2 of MAGT3 gene was flanked with two loxP sites. The targeting construct was microinjected into embryonic stem cells of C57BL/6 background mice. Heterozygous mice were generated by standard procedures with *in vivo* Cre-mediated excision of loxP-neo-loxP cassette. MGAT3 and/or loxP insert were amplified by PCR using primers 5'-AAGTTGGATACAGTGGAGGGCTAG-3' and 5'-CACTGACCTTAATGTTCTTTCTTGGAC-3'. Conditional deletion of *MGAT3* gene was accomplished by crossbreeding leptin receptor (*LepR*)-*Cre* transgenic mice (donated by Prof. Caiwen Duan, Dept. of Pharmacology and Chemical Biology, Shanghai Jiao Tong University) with *MGAT3*$^{fl/fl}$ mice. Animal

experiments were approved by the Animal Care and Use Committee of Northwest University, and performed in accordance with its guidelines.

Isolation and culture of mouse BM stromal cells

Mouse BM stromal cells were isolated from tibia and femoral marrow, and cultured for 24 h in minimal essential medium alpha (MEMα; Biological Industries) added with 10% FBS and 1% penicillin/streptomycin (Beyotime) at 37°C in 5% CO_2 atmosphere. Culture medium was changed every 3 days. Cells with hematopoietic markers were removed, and CD54, CD73, and CD90 expression was evaluated in adherent cells.

Human BM stromal cells

Human BM stromal cells were isolated from marrow aspirates from healthy subjects or MDS/AML patients (People's Hospital of Shaanxi Province) (Table S1). Briefly, mononuclear cells were separated by Ficoll-Hypaque gradient centrifugation. Primary BM stroma cells were isolated from Ficoll-Hypaque–separated bone marrow mononuclear cells by culturing 2.5 to 3 × 10^7 cells per T75 flask in DMEM F12 (Biological Industries) cultured at 37°C with 5% CO_2. After 3 days, non-adherent cells were removed. When cultures reached 80–90% confluence, cells were detached, and plated for following experiments. Written informed consent was obtained from all marrow donors in accordance with Declaration of Helsinki guidelines. All experimental designs using human tissues were reviewed and approved by the Research Ethics Committee of Northwest University.

Stable transfection of MGAT3

MGAT3 was amplified via PCR and linked to lentiviral vector pLVX-AcGFP-N1 (Takara; Shiga, Japan). Lentiviral vectors encoding short hairpin RNAs (shRNAs) targeting MGAT3 were generated using piLenti-siRNA. Scrambled piLenti-siRNA was used as negative control. Constructed lentiviral vectors, together with pMD2.G and psPAX2 (Addgene; Cambridge, MA, USA), were packed into HEK293T cells. HS27a and HS5 cells were infected with lentivirus particles. Stable transfectants were selected using puromycin and confirmed by western blotting.

Immunofluorescence staining

Cells cultured on confocal small dishes were washed with PBS, fixed with 4% paraformaldehyde (Sigma-Aldrich; St. Louis, MO, USA) in PBS for 15 min, permeabilized with 0.2% Triton X-100 in PBS for 10 min, incubated with 3% BSA in PBS at 37°C for 1 h, probed with primary antibody against MGAT3 (cat # ab75769, Abcam; Cambridge, MA, USA) or MCAM (cat # ab135514, Abcam) at 4°C overnight, incubated 1 h with FITC-conjugated anti-rabbit IgG antibody (Abcam), washed 3x with PBS, and incubated with DAPI for 15 min at room temperature (RT). For lectin staining, cells were fixed, blocked as described above, and probed with FITC-conjugated lectin PHA-E (Vector Laboratories; Burlingame, CA, USA). Fluorescence images were obtained by confocal microscopy (model TCS SP8, Leica Microsystems; Solms, Germany).

Quantitative real-time PCR (qRT-PCR)

Total RNA was isolated using RNA Pure Tissue & Cell Kit (CW Biotech; Beijing). Primers were designed using Primer-BLAST software program (ncbi.nlm.nih.gov/tools/primer-blast). First-strand cDNA was synthesized from total RNA using HiScript II Q RT SuperMix (Vazyme; Nanjing, China). qRT-PCR was performed by SYBR Green I dye detection with AceQ qPCR SYBR Green Master Mix (Vazyme), Primers are listed in Online Supplementary Table 2. and gene expression was quantified by $2^{-\Delta\Delta Ct}$ method [18, 19].

In vitro co-culture model

HS5 and HS27a cells (1×10^5) were seeded in 6-well plates and cultured overnight in RPMI 1640 supplemented with 10% FBS. Clonal cells (3×10^5) were added for co-culture, incubation continued for 48 h, and stromal and clonal cells were collected.

Flow cytometry (FACS) analysis

Cells were co-cultured with stromal cells for 48 h, harvested, washed, fixed, permeabilized, and incubated with FITC-conjugated PHA-E for 2 h at 37°C. MDS/AML malignant clonal cells were distinguished from co-cultured cells using FITC-conjugated anti-human CD45 Ab (BD Biosciences; Franklin Lakes, NJ, USA). For proliferation analysis, cells were stained with EdU Alexa Fluor 647 kit (Keygen; Jiangsu, China) as per manufacturer's protocol, and analyzed by FACS (ACEA Biosciences; San Diego, CA, USA).

Western blotting

Cells were harvested and lysed with radioimmunoprecipitation assay (RIPA) buffer (50 mM Tris, pH 7.2, 1% Triton X-100, 0.5% sodium deoxycholate, 0.1% SDS, 150 mM NaCl, 10 mM $MgCl_2$, 5% glycerol) containing 1% protease inhibitor (Sigma-Aldrich). Lysate was centrifuged (14,000 × *g*, 15 min, 4°C), supernatant was collected, and protein concentration was determined by bicinchoninic acid (BCA) assay (Beyotime). Proteins (25 μg) were separated by SDS-PAGE, and transferred onto polyvinylidene difluoride (PVDF) membranes (Bio-Rad; Hercules, CA, USA). Membranes were blocked with 3% BSA (Beyotime) in TBST for 1 h at 37°C, probed overnight with primary antibody at 4°C, and incubated with appropriate HRP-conjugated secondary antibody. Bands were visualized by enhanced chemiluminescence (ECL; Vazyme), and photographed using a bioluminescence imaging system (Tanon; Shanghai).

Lectin blotting

Proteins from each sample were separated by 8% SDS-PAGE and transferred onto PVDF membranes. Membranes were soaked in 3% (w/v) BSA in TBST for 2 h at 37°C, probed with biotin-conjugated PHA-E (Vector Labs) overnight at 4°C, and incubated with appropriate HRP-conjugated streptavidin. Bands were visualized and photographed as described above.

Purification and characterization of exosomes

Exosomes were purified from plasma or cells and characterized as described previously [20]. For cells, KG1a cells were cultured with RPMI 1640 containing 10% exosome-free FBS for 48 h, and supernatant was collected. For patient or healthy control, 5 mL bone marrow aspirate was collected in EDTA-

anticoagulant tube, and centrifuged at 2000 x g for 20 min at 4°C, using bone marrow sample separation kit (TBD; Tianjin, China). 1 mL upper plasma was collected. Cell supernatant or plasma was centrifuged sequentially at 500 × *g* for 10 min, 2000 × *g* for 20 min, 10,000 × *g* for 30 min at 4°C, and ultracentrifuged twice at 100,000 × *g* (model Optima XE-100, Beckman Coulter Life Sciences; Indianapolis, IN, USA) for 70 min. Morphology of exosomes was evaluated by transmission electron microscopy (model H-7650; Hitachi; Tokyo) at 80 kV, and size distribution evaluated by nanoparticle tracking analyzer (NanoSight LM10, (Malvern Instruments; Malvern, UK).

Exosome uptake

Purified exosomes were labeled with ExoTracker probes as described previously[21]. In brief, exosomes were incubated with ExoTracker for 30 min at 37°C, unbound ExoTracker removed using 10-kD centrifugal ultrafiltration filters, and cells incubated with labeled exosomes for 2 h at 37°C and analyzed by FACS.

Exosomal miRNA-seq analysis

Total RNA from exosomes was extracted using exoRNeasy Serum/ Plasma Maxi Kit (Qiagen; Valencia, CA, USA) as per manufacturer's instructions. miRNA libraries were constructed using QIAseq miRNA Library Kit (Qiagen) and analyzed using automated DNA analyzer (model Qsep100, BiOptic Inc.; Taiwan). miRNA-seq analysis was performed using NextSeq CN500 system (Illumina; San Diego, CA, USA).

Luciferase reporter assay

Sequences of predicted miR-188-5p binding sites of MGAT3 3'-untranslated regions (3'-UTRs), and corresponding mutants, were synthesized and inserted into luciferase reporter vector psiCHECK-2 (Promega; Madison, WI, USA). Constructed plasmids were co-transfected together with miR-188-5p mimic into HEK293T cells. Relative luciferase activity was determined using Dual Luciferase Assay Kit (Promega) as per manufacturer's instructions.

Immunoprecipitation (IP) assay

Cells from each sample were cultured and lysed as described above. Lysates (1 mg) were incubated with 2 µg primary antibody for 1 h at 4°C, and added with 20 µl protein A/G Plus-Agarose. The mixture was incubated on a shaker overnight at 4°C, rinsed with 1X PBS, denatured with SDS sample loading buffer, and analyzed by western blotting.

Proteomic analysis

Proteins (100 µg) were denatured with 8 M urea, reduced by 5 mM dithiothreitol (DTT) for 1 h at RT, alkylated with 20 mM iodoacetamide (IAM) for 30 min in the dark at RT, diluted with deionized water to lower urea concentration below 2 M, digested with lysyl endopeptidase (Wako Puro Chemical; Osaka, Japan) for 4 h at 37°C, and digested with trypsin (Promega) overnight at 37°C. The mixture was acidified with 10% trifluoroacetic acid (TFA) to pH < 3 and purified using C18 cartridges (Waters Corp.; Taunton, MA, USA). Two-dimensional liquid chromatography/ mass spectrometry (LC-MS) and data analysis were

performed using LTQ Orbitrap MS (Thermo Fisher; San Jose, CA, USA) and Proteome Discoverer software tool (Thermo Fisher), with quantification by MaxQuant software program V. 1.5.2.8 (maxquant.org).

Immunoprecipitation MS (IP-MS)

Protein extraction, IP, and SDS-PAGE were performed as described previously[22]. Protein bands were stained with Coomassie Brilliant Blue R-250 (Thermo Fisher) and then decolorized. Target bands were diced into small pieces, destained with 25 mM NH_4HCO_3 in 50% acetonitrile (ACN), reduced by 10 mM DTT/ 50 mM NH_4HCO_3 for 1 h at RT, alkylated with 20 mM IAM/ 50 mM NH_4HCO_3 in the dark for 45 min, and digested with trypsin overnight at 37°C. Digested peptides were dissolved with 60% ACN/ 0.1% TFA and subjected to 2-D LC-MS analysis (Thermo Fisher).

NHS-LC-biotin labeling of membrane proteins

Cells were washed with cold PBS to remove amine-containing medium, resuspended in 2 mM EZ-Link Sulfo-NHS-LC-Biotin (Thermo Fisher), and incubated for 30 min at RT. Excess biotinylation reagent was neutralized by 100 mM glycine in PBS for 15 min at RT. For each sample, total protein was extracted, and biotin-labeled membrane protein was pulled down by streptavidin-coupled agarose beads and assayed by western blotting.

In vivo mouse experiment

Nod.cg-Prkdc^{scid} Il2rg^{tm1wjll} (NSG) mice (age 6–8 wk) were i.p. injected with the chemotherapy drug busulfan (30 mg/kg) to suppress BM activity. HS5, HS5-MCAM, or HS5-MCAM-Mu cells together with KG1a cells (ratio 1:3) were co-transplanted into mice via tail vein on day 1. Peripheral blood was collected and assayed on days 10, 17, and 24, and mononuclear cells were stained with anti-CD45 Ab for FACS analysis. Mice were then euthanized, and spleen and BM were collected. All animal experiments were performed in accordance with guidelines of the Animal Care and Use Committee of Northwest University.

Statistical analysis

Data are presented as mean ± SEM. Statistical significance of differences between means of two groups was evaluated by Student's t-test. Comparisons of multiple groups were evaluated by ANOVA with Bonferroni's post hoc test.

Results

Levels of bisecting GlcNAc and MGAT3 in BM stromal cells

Expression of bisecting GlcNAc and its glycosyltransferase MGAT3 were examined in primary BM stromal cells (Fig. 1A). MGAT3 expression at transcriptional level was significantly lower for MDS/AML patients than healthy subjects (Fig. 1B). Confocal microscopy likewise revealed that bisecting GlcNAc and MGAT3 levels were significantly lower for MDS/AML patients than healthy subjects (Fig. 1C). Bisecting GlcNAc expression in stromal cells was significantly downregulated by co-culture with KG1a or SKM-1 myeloid

cells (Fig. 1D), as confirmed by FACS analysis (Fig. 1E). These findings, taken together, demonstrate aberrant expression of bisecting GlcNAc in MDS/AML stromal cells, and the ability of myeloid cells to alter N-glycosylation levels of niche cells.

Effect of bisecting GlcNAc in stroma on myeloid cell proliferation

Normal BM stroma (termed NBM stroma) was treated with forskolin, an adenylyl cyclase activator that stimulates MGAT3 expression[23]. This treatment resulted in clear enhancement of bisecting GlcNAc level (Fig. 2A). Proliferation of KG1a or SKM-1 cells co-cultured with forskolin-treated NBM stroma (in comparison with nontreated stroma) was reduced (Fig. 2B). By introducing MGAT3 into HS27a, we established a stable transfectant (termed HS27a-M3) that expressed high bisecting GlcNAc level (Fig. 2C). Co-culture of KG1a or SKM-1 with HS27a-M3 resulted in reduced proliferation (Fig. 2D). Similarly, co-culture of KG1a or SKM-1 with an MGAT3-knockdown version of HS5 (termed HS5-shM3) (Fig. 2E) also resulted in enhanced proliferation (Fig. 2F). These findings demonstrate that upregulation of bisecting GlcNAc level in stroma induced by MGAT3 overexpression inhibited myeloid cell proliferation, and conversely myeloid cell proliferation was enhanced by downregulation of bisecting GlcNAc level.

We generated *LepR-Cre; MGAT3*$^{fl/fl}$ mice in order to investigate the functional role of bisecting GlcNAc in the BM niche *in vivo* (Fig. 2G). These mice showed strongly reduced expression of MGAT3 and stromal bisecting GlcNAc (Fig. 2H), retarded growth relative to *MGAT3*$^{fl/fl}$ (Fig. 2I), and development of severe anemia and thrombocytopenia (although WBC counts were comparable to those of *MGAT3*$^{fl/fl}$) (**Fig. S1**). KG1a cells grew well when transplanted into *L*epR-Cre; MGAT3$^{fl/fl}$ (Fig. 2J). These findings illustrate substantial effects on the hematopoietic microenvironment of MGAT3 expression and bisecting GlcNAc production in BM stroma.

Exosomal miR-188-5p of myeloid cells suppresses stromal bisecting GlcNAc level

Exosomes are packaged with bioactive proteins, lipids, or nucleic acids, and help mediate cell-cell communication[24]. We purified exosomes from KG1a by differential centrifugation in order to investigate regulation by myeloid cells on stromal bisecting GlcNAc expression. The purified exosomes showed clear expression of exosome markers such as CD63, Alix, and TSG101 (Fig. 3A), with narrow size distribution around 100 nm (Fig. 3B), and sphere-like morphology (Fig. 3C). They were efficiently taken up by NBM stroma (Fig. 3D).

Co-culture of HS5, HS27a, or primary NBM stroma with KG1a cells, or treatment with KG1a-derived exosomes, resulted in significant reduction of MGAT3 expression at mRNA and protein levels (Fig. 3E, F), and of bisecting GlcNAc levels (Fig. 3F). miRNA-seq analysis identified 1671 micro-RNAs (miRs) in KG1a-derived exosomes (data not shown). These findings, in combination with TargetScan and miRBD analyses, led to prediction of 52 MGAT3-targeting miRs among KG1a exosomal miRs (Fig. 3G). MGAT3

levels in these miRs showed negative correlation with miR188-5p expression in AML and pan-cancer samples in The Cancer Genome Atlas (TCGA) database (Fig. 3H, I**)**. Kaplan-Meier analysis showed significant correlation of overall AML patient survival with miR-188-5p expression (Fig. 3J). miR-188-5p expression was notably higher in exosomes derived from plasma of MDS or AML patients, vs. healthy subjects (Fig. 3K).

We hypothesized, based on the above observations, that miR-188-5p from KG1a exosomes suppresses bisecting GlcNAc levels by targeting MGAT3. Transient transfection of miR-188-5p inhibitor into KG1a cells, significantly increased MGAT3 and bisecting GlcNAc expression in co-cultured stroma (**Fig. S2A, B)**. MGAT3 and bisecting GlcNAc expression in HS27a or primary stroma were downregulated by co-culture with KG1a, but restored by treatment with miR-188-5p inhibitor (Figs. 3L, S2C). Conversely, transient transfection of miR-188-5p mimic into HS5, HS27a, or primary stroma led to downregulation of MGAT3 and bisecting GlcNAc expression (Figs. 3M, S2D). Luciferase reporter assay revealed direct binding of miR-188-5p to 3'-UTR of MGAT3, but not to mutated 3'-UTR (Fig. 3N). These findings indicate that exosomal miR-188-5p from myeloid cells (KG1a) reduced stromal bisecting GlcNAc levels by targeting and silencing MGAT3 gene.

Proteomic analysis of bisecting GlcNAcylated proteins in BM stroma

We then performed quantitative proteomic analysis in order to identify differentially expressed proteins affected by bisecting GlcNAc modification in BM stroma. Stromal proteins from *LepR-Cre; MGAT3$^{fl/fl}$* and *MGAT3$^{fl/fl}$* mice were denatured, alkylated, digested, and analyzed by triplicate LC-MS/MS (Fig. 4A). 3329 proteins were identified in stroma from control (CON) and conditional knockout (cKO) mice, as presented by Volcano blot (Fig. 4B). 380 differentially expressed proteins (criteria: fold change > 1.5 or < 0.67; $p < 0.05$) were identified; they consisted of 190 upregulated and 190 downregulated proteins (heatmap shown in Fig. 4C). Gene Ontology (GO) classification and KEGG pathway analyses of these proteins indicated close association with cell-cell adhesion and oxidation-reduction (redox) processes (**Fig. S3)**.

Expression of MCAM, a typical adhesion molecule that supports hematopoietic cell growth, was significantly increased in *LepR-Cre; MGAT3$^{fl/fl}$* (Fig. 4D). Western blotting revealed downregulated bisecting GlcNAc expression and upregulated MCAM expression in stroma from cKO mice (Fig. 4E). MCAM expression in BM stroma was higher for MDS or AML patients than for healthy subjects (Fig. 4F, G).

We hypothesized, in view of these findings, that MCAM expression is affected by modification of stromal bisecting GlcNAc level. MCAM expression was upregulated in HS5-shM3 but downregulated in HS27a-M3, consistently with this hypothesis (Fig. 4H). We cloned MGAT3 gene into a tetracycline-inducible gene expression system and transfected it into HS27a (HS27a-TetOne-MGAT3). Treatment of these cells with doxycycline (dox) resulted in gradual, time-dependent increase of MGAT3 expression, and decrease of MCAM and bisecting GlcNAc expression (Fig. 4I). Introduction or silencing of MGAT3 in primary stroma

led respectively to down- and up-regulation of MCAM expression (Fig. 4J). These findings demonstrate that MCAM expression in stromal cells was regulated by bisecting GlcNAc modification.

Identification and function of bisecting GlcNAc modification sites on MCAM

Increase of bisecting GlcNAc levels did not alter MCAM expression at the mRNA level (data not shown), suggesting that modulation of MCAM expression by bisecting GlcNAc modification is a posttranslational event. MCAM is a typical transmembrane glycoprotein, and we accordingly used Sulfo-NHS-LC-Biotin to label MCAM on cell membrane (Fig. 5A). Total MCAM content was much lower in HS27a-M3 than in HS27a cells (Fig. 3G, and confirmed in these experiments). In HS27a-M3, relative to HS27a, biotin-labeled MCAM level on cell membrane was lower, whereas MCAM level in cytoplasm was higher (Fig. 5B). Blocking of cytosolic protein synthesis by cycloheximide accelerated MCAM degradation (Fig. 5C). In most cases, intracellular proteins are degraded via ubiquitin-proteasome pathways, whereas extracellular proteins and cell surface proteins enter cells by endocytosis and are degraded via lysosomal pathways[25–27]. MCAM expression in HS27a-M3 was enhanced by treatment with lysosomal inhibitor chloroquine, but unaffected by treatment with proteasome inhibitor MG132 (Fig. 5D). MCAM in HS27a-M3 was shown by confocal microscopy to be localized mainly in lysosomes (Fig. 5E). These findings indicate that bisecting GlcNAc modification affects MCAM stability, and causes MCAM degradation via a lysosomal pathway.

In order to identify bisecting GlcNAc modification sites on MCAM, bisecting GlcNAc-modified MCAM was IP'd using anti-MCAM antibody, converted to tryptic peptides, and subjected to intact glycoproteomic analysis. We identified unique peptide GLSQSQGN#LSHVDWFSVHK of bisecting GlcNAc-modified MCAM, characterized by pep + HexNAc3Hex1 (Fig. 5F). Based on location of bisecting GlcNAc modification site at Asn 56, we established wild-type MCAM-overexpressing cells (termed HS5-MCAM), and generated a glycosylation-deficient N56D mutant of HS5 (termed HS5-MCAM-Mu). Forced expression of either MCAM or MCAM-Mu in HS5 resulted in nearly identical MCAM levels (Fig. 5G). MCAM was rarely modified with bisecting GlcNAc in HS5-MCAM-Mu, as confirmed by IP assay with PHA-E (Fig. 5H). These findings indicate that Asn 56 is the major bisecting GlcNAc modification site.

Mutation of bisecting GlcNAc modification site had no effect on MCAM expression at protein or mRNA levels (Figs. 5G, S4B). However, MCAM level on cell membrane was significantly lower in HS5-MCAM-Mu than in HS5-MCAM (**Fig. S4C**). Similarly, when MCAM was pulled down by Sulfo-NHS-LC-Biotin strategy as described above, MCAM level was significantly lower in HS5-MCAM-Mu than in HS5-MCAM (Fig. 5H). For the two cell types, MCAM expression was assayed in total cell lysates, on cell membrane, and in cytoplasm. In HS5-MCAM-Mu, relative to HS5-MCAM, MCAM level was lower on cell membrane, and higher in cytoplasm (**Fig. S4D**). For HS5-MCAM-Mu, cycloheximide treatment to block novel cytosolic protein synthesis accelerated MCAM degradation (**Fig. S4E**), while MCAM expression was enhanced by chloroquine treatment and unaffected by MG132 treatment (Fig. 5I). MCAM in HS5-MCAM-Mu was shown by confocal microscopy to be localized in lysosomes (Fig. 5J). Thus, localization of MCAM on cell

membrane could be reduced by either removal of N-glycan structures at Asn 56 by mutation, or enhanced bisecting GlcNAc modification at this site. These findings indicate that stable localization of MCAM on cell membrane depends on certain N-glycan structures, but not on bisecting GlcNAc at Asn 56.

Effect of MCAM on myeloid cell proliferation

In vivo and *in vitro* experiments were performed to evaluate effects of mutation of Asn 56 (bisecting GlcNAc modification site on MCAM) on myeloid cell function. Proliferation of myeloid cells co-cultured with HS5-MCAM increased, whereas that of cells co-cultured with HS5-MCAM-Mu declined to the level of cells co-cultured with HS5 (Figs. 6A, B; S5). MCAM on cell membrane evidently supports myeloid cell proliferation.

Based on the above finding, transplantation experiments were performed to clarify the *in vivo* role of bisecting GlcNAc modification of MCAM in myeloid cell proliferation (Fig. 6C). Proportion of KG1a cells in peripheral blood of NSG mice was significantly higher when KG1a were co-injected with HS5-MCAM cells, relative to co-injection with HS5 or HS5-MCAM-Mu (Fig. 6D, E). Expression in BM and spleen of $CD45^+$ signal, a myeloid cell marker, was shown by immunohistochemical analysis to be significantly lower for HS5-MCAM-Mu co-injected relative to HS5-MCAM co-injected group (Fig. 6F-H). These findings indicate that the supportive effect of stromal cells on myeloid cell proliferation was disrupted in glycosylation-deficient N56D mutant of HS5 because of reduced MCAM expression on stromal cell membrane.

Membrane proteins involved in myeloid cell interaction with MCAM

To clarify the molecular mechanism underlying the effect of MCAM Asn 56 glycosylation on myeloid cell proliferation, we performed IP-MS to identify membrane proteins on KG1a that interact with MCAM on stromal cells (Fig. 7A). 163 differentially expressed proteins were identified (Fig. 7B), and those that interacted with MCAM on KG1a were subjected to systematic proteomic analysis (Fig. 7C). Among the 29 overlapping proteins that interacted with MCAM in HS5-MCAM, in HS5-MCAM-Mu, and in interactome from string database[28], CD13, a human myeloid plasma membrane glycoprotein (also known as gp150), was identified. CD13 was shown by co-IP assay to bind more strongly to wild-type MCAM than to mutant MCAM (Fig. 7D). To rule out the possibility that MCAM-bound CD13 is derived mainly from KG1a rather than stromal cells, we knocked down CD13 expression in HS5-MCAM and HS5-MCAM-Mu (Fig. 7E). Binding to CD13 in KG1a cells was strong for wild-type MCAM in stromal cells, but weak for mutant MCAM (Fig. 7F).

Activated CD13 has been reported to facilitate cell proliferation by inducing extracellular signal-regulated kinase (ERK) phosphorylation[29]. We therefore pretreated KG1a cells with the aminopeptidase inhibitor bestatin, a specific inhibitor of CD13, to block CD13 on cell membrane. ERK signaling was activated in KG1a co-cultured with HS5-MCAM, but clearly suppressed in KG1a co-cultured with HS5-MCAM-Mu, and in bestatin-pretreated KG1a co-cultured with HS5-MCAM (Fig. 7G). Similarly, KG1a proliferation was

significantly enhanced by co-culture with HS5-MCAM, but suppressed by co-culture with HS5-MCAM-Mu or with HS5-MCAM in combination with bestatin treatment(Fig. 7H).

These findings, taken together, demonstrate that MCAM on stromal cells binds to CD13 on myeloid cells, activates ERK signaling, and promotes myeloid cell growth.

Discussion

BM stroma is a heterogeneous assembly of cells that provide structural and physiological support for hematopoietic cells. Abnormal hematopoiesis may result from genetic dysregulation, or from a dysfunctional structure acting by itself or affecting crosstalk with hematopoietic stem cells[30]. Many factors are involved in crosstalk between stroma and hematopoietic cells; among these, glycoconjugates (glycoproteins, glycolipids, and glycosaminoglycans), play key roles in modulating functions of HSPCs in BM[31–33].

Glycoconjugates form a thin polysaccharide matrix layer, termed glycocalyx, on cell membranes. Glycocalyx affects nearly all interactions between cells and their surrounding environment. Several glycoengineering strategies have been developed to improve homing and engraftment of cells following hematopoietic stem cell transplantation[34–36]. An example is forced *ex vivo* fucosylation of $CD34^+$ cells to improve HSPC homing to BM, resulting in enhanced neutrophil and platelet engraftment [37]. In this study, we observed downregulated levels of bisecting GlcNAc and its glycosyltransferase MGAT3 in BM stroma of MDS or AML patients. Bisecting GlcNAcylation is a specific type of N-glycosylation that affects adhesion, migration, and other cellular functions by modifying adhesion molecules and receptors (notably E-cadherin, integrins, tetraspanins, and EGFR)[17, 38, 39]. Bisecting GlcNAc is also involved in organ growth and development[40]. Low bisecting GlcNAc levels in stromal cells promote proliferation of hematopoietic clonal cells. Malignant clonal cells were shown to package miR-188-5p into exosomes for delivery to recipient stromal cells, where it reduced MGAT3 expression and bisecting GlcNAc level. These and similar findings demonstrate the ability of malignant cells to reprogram their microenvironment[41].

We identified MCAM as a bisecting GlcNAc-bearing target protein in stromal cells by MS analysis of glycoproteins in combination with PHA-E enrichment. MCAM was originally identified in human melanoma as a 113-kDa glycoprotein belonging to the immunoglobulin (Ig) superfamily of cell adhesion molecules[42]. It was subsequently shown to be highly expressed in other tumors and in endothelial cells. MCAM plays functional roles in a variety of cellular processes, including transendothelial migration, proliferation, and cancer metastasis[43–45]. The previous findings show that MCAM is a useful marker associated with BM niche, together with LepR[46]. MCAM overexpression in mesenchymal stromal cells (MSCs) enhanced adhesion of HSPCs to MSCs, and supported HSPC growth. In contrast, silencing of MCAM in MSCs suppressed HSPC proliferation, and strongly reduced formation of long-term culture-initiating cells[47]. Our 2013 study indicated that high MCAM expression in stromal cells facilitated engraftment of cloned MDS patient cells in a mouse xenotransplantation model[13]. Consistently with the

finding by P. Bianco's group of high MCAM expression in MDS or AML patients[48], we observed that high MCAM expression in stromal cells supported myeloid cell proliferation *in vitro* and *in vivo*.

N-glycosylation plays essential roles in protein folding and trafficking, and whole N-glycosylation knockdown or mutation at certain N-glycosylation sites resulted in misfolding, mis-distribution, instability, and/or degradation of such glycoproteins as glucose transporter GLUT4, human tripeptidyl-peptidase I, and dopamine transporter [49–51]. MCAM expression was strongly enhanced when bisecting GlcNAc level was low, reflecting a close association of bisecting GlcNAc modification with MCAM expression. When bisecting GlcNAc level was high, MCAM content in membranes was significantly decreased and localization of MCAM in lysosomes was increased. Bisecting GlcNAc appeared to modulate MCAM translocation to cell membrane, and to induce degradation of MCAM via lysosomal pathways. IP-MS analysis identified Asn 56 on MCAM as the key bisecting GlcNAc-bearing site. Promoting effect on malignant clonal cell proliferation *in vitro* and *in vivo* was weaker for glycosylation-deficient N56D mutant of HS5 (HS5-MCAM-Mu) than for HS5-MCAM. Knockdown of N-glycosylation at Asn 56 reduced MCAM localization on cell membrane, indicating that such localization depends on other N-glycan structures not yet identified.

In regard to functional mechanism, we found that MCAM on stromal cell membrane supported malignant clonal cell growth through interaction with the transmembrane aminopeptidase CD13. CD13 is frequently overexpressed in tumor cells, is involved in angiogenesis and cancer progression[52], and is widely expressed in cells of the myeloid (HSPC) lineage[53, 54]. $CD13^+$ myeloid BM-derived cells (BMDCs) promote angiogenesis and vascular maturation by regulating pericyte recruitment through increased production of MCP-1 and MMP-9[55]. $CD13^+$ myeloid BMDCs in the tumor microenvironment are therefore a potential target for antiangiogenic therapeutics[56]. We observed that elimination of bisecting GlcNAc on MCAM by Asn 56 mutation, or by bestatin treatment, notably reduced CD13 binding, inactivated ERK signaling, and suppressed myeloid cell growth. The supportive function of stroma on clonal cell growth therefore appears to depend on interaction between MCAM on stromal cells and CD13 on clonal cells.

In conclusion, our findings support the concept that glycocalyx on cell membranes is the first responsive barrier between BM stroma and myeloid cells. MDS/AML clonal cells can modify bisecting GlcNAc levels of BM stroma through exosome secretion, thereby promoting malignant clonal cell proliferation and survival, and suppressing normal hematopoiesis (Fig. 8). Treatment with drugs that specifically target MDS/AML clonal cells may help repair a damaged BM niche and thereby eliminate a potential pathway for disease recurrence. Novel therapeutic strategies that restore a healthy BM niche, based on glycosylation modification, may show improved effectiveness against MDS/AML and similar disorders.

Declarations

Author contributions

XL and FG conceived and devised the study. FG, XL, JF, and YW designed the experiments and analytical procedures. JF, BL, XY, XZ, QC, JG,and YZ performed experiments. YW provided clinical samples. YZ, ZT, LL, JW, HL and ZD performed bioinformatics, data analysis, and statistical analysis. FG and XL supervised research and wrote the manuscript. All authors read and approved the final manuscript.

Acknowledgments

The authors are grateful to Dr. S. Anderson for English editing of the manuscript.

Competing Interests

The authors declare no conflict of interest, or competing financial interest.

References

1. S. J. Morrison & D. T. Scadden. The bone marrow niche for haematopoietic stem cells. Nature 2014; **505**: 327–34.
2. M. S. Shafat, B. Gnaneswaran, K. M. Bowles & S. A. Rushworth. The bone marrow microenvironment - Home of the leukemic blasts. Blood Rev 2017; **31**: 277–286.
3. S. Snykers, J. De Kock, V. Rogiers & T. Vanhaecke. In vitro differentiation of embryonic and adult stem cells into hepatocytes: state of the art. Stem Cells 2009; **27**: 577–605.
4. J. Corre, et al. Bone marrow mesenchymal stem cells are abnormal in multiple myeloma. Leukemia 2007; **21**: 1079–1088.
5. J. E. Noll, et al. Myeloma plasma cells alter the bone marrow microenvironment by stimulating the proliferation of mesenchymal stromal cells. Haematologica 2014; **99**: 163–171.
6. M. S. Shafat, et al. Leukemic blasts program bone marrow adipocytes to generate a protumoral microenvironment. Blood 2017;**129**: 1320–1332.
7. A. Capela & S. Temple. LeX/ssea-1 is expressed by adult mouse CNS stem cells, identifying them as nonependymal. Neuron 2002;**35**: 865–875.
8. W. C. Wu, et al. Circulating hematopoietic stem and progenitor cells are myeloid-biased in cancer patients. Proc Natl Acad Sci U S A 2014; **111**: 4221–4226.
9. H. Hemmoranta, et al. N-glycan structures and associated gene expression reflect the characteristic N-glycosylation pattern of human hematopoietic stem and progenitor cells. Exp Hematol 2007; **35**: 1279–1292.
10. A. B. Mak, et al. CD133 protein N-glycosylation processing contributes to cell surface recognition of the primitive cell marker AC133 epitope. J Biol Chem 2011; **286**: 41046–41056.
11. K. D. Marjon, et al. Tetraspanin CD82 regulates bone marrow homing of acute myeloid leukemia by modulating the molecular organization of N-cadherin. Oncogene 2016; **35**: 4132–4140.
12. E. E. Irons, et al. B cells suppress medullary granulopoiesis by an extracellular glycosylation-dependent mechanism. Elif 2019; **8**: e47328.

13. X. Li, A. M. Marcondes, T. Ragoczy, A. Telling & H. J. Deeg. Effect of intravenous coadministration of human stroma cell lines on engraftment of long-term repopulating clonal myelodysplastic syndrome cells in immunodeficient mice. Blood Cancer J 2013; **3**: e113.
14. X. Li, et al. Quantitative analysis of glycans, related genes, and proteins in two human bone marrow stromal cell lines using an integrated strategy. Exp Hematol 2015; **43**: 760–769.
15. J. Li, et al. MGAT3-mediated glycosylation of tetraspanin CD82 at asparagine 157 suppresses ovarian cancer metastasis by inhibiting the integrin signaling pathway. Theranostics 2020; **10**: 6467–6482.
16. L. Cheng, et al. Bisecting N-Acetylglucosamine on EGFR Inhibits Malignant Phenotype of Breast Cancer via Down-Regulation of EGFR/Erk Signaling. Front Oncol 2020; **10**: 929.
17. Z. Tan, et al. Bisecting GlcNAc modification diminishes the pro-metastatic functions of small extracellular vesicles from breast cancer cells. Journal of extracellular vesicles 2020; **10**: e12005.
18. J. Ribeiro, et al. P53 deregulation in Epstein-Barr virus-associated gastric cancer. Cancer Lett. 2017; **404**: 37–43.
19. K. B. Shah, S. D. Chernausek, A. M. Teague, D. E. Bard & J. B. Tryggestad Maternal diabetes alters microRNA expression in fetal exosomes, human umbilical vein endothelial cells and placenta. Pediatr Res 2021; **89**: 1157–1163.
20. Z. Tan, et al. Bisecting GlcNAc modification diminishes the pro-metastatic functions of small extracellular vesicles from breast cancer cells. J Extracell Vesicles 2020; **10**: e12005.
21. X. Zhou, et al. ExoTracker: a low-pH-activatable fluorescent probe for labeling exosomes and monitoring endocytosis and trafficking. Chemical communications 2020; **56**: 14869–14872.
22. M. Scharf, et al. A Spectrum of Neural Autoantigens, Newly Identified by Histo-Immunoprecipitation, Mass Spectrometry, and Recombinant Cell-Based Indirect Immunofluorescence. Frontiers in immunology 2018; **9**: 1447.
23. A. S. Sultan, et al. Bisecting GlcNAc structures act as negative sorting signals for cell surface glycoproteins in forskolin-treated rat hepatoma cells. J Biol Chem 1997; **272**: 2866–2872.
24. M. Negahdaripour, et al. Small extracellular vesicles (sEVs): discovery, functions, applications, detection methods and various engineered forms. Expert opinion on biological therapy 2021; **21**: 371–394.
25. J. Zhou, et al. A novel autophagy/mitophagy inhibitor liensinine sensitizes breast cancer cells to chemotherapy through DNM1L-mediated mitochondrial fission. Autophagy 2015; **11**: 1259–1279.
26. J. Jia, et al. AMPK, a Regulator of Metabolism and Autophagy, Is Activated by Lysosomal Damage via a Novel Galectin-Directed Ubiquitin Signal Transduction System. Mol Cell 2020; **77**: 951–969.
27. Y. Wang, et al. Lysosome-associated small Rab GTPase Rab7b negatively regulates TLR4 signaling in macrophages by promoting lysosomal degradation of TLR4. Blood 2007; **110**: 962–971.
28. D. Szklarczyk, et al. STRING v10: protein-protein interaction networks, integrated over the tree of life. Nucleic acids research 2015; **43**: 447–52.

29. J. Subramani, et al. Tyrosine phosphorylation of CD13 regulates inflammatory cell-cell adhesion and monocyte trafficking. Journal of immunology 2013; **191**: 3905–3912.
30. S. Yehudai-Resheff, et al. Abnormal morphological and functional nature of bone marrow stromal cells provides preferential support for survival of acute myeloid leukemia cells. International journal of cancer 2019; **144**: 2279–2289.
31. S. Klamer & C. Voermans. The role of novel and known extracellular matrix and adhesion molecules in the homeostatic and regenerative bone marrow microenvironment. Cell adhesion & migration 2014; **8**: 563–577.
32. S. M. Crean, et al. N-linked sialyated sugar receptors support haematopoietic cell-osteoblast adhesions. British journal of haematology 2004; **124**: 534–546.
33. A. Buffone & V. M. Weaver. Don't sugarcoat it: How glycocalyx composition influences cancer progression. The Journal of cell biology 2020; **219**.
34. J. Lee, et al. mRNA-mediated glycoengineering ameliorates deficient homing of human stem cell-derived hematopoietic progenitors. The Journal of clinical investigation 2017;**127**: 2433–2437.
35. B. Dykstra, et al. Glycoengineering of E-Selectin Ligands by Intracellular versus Extracellular Fucosylation Differentially Affects Osteotropism of Human Mesenchymal Stem Cells. Stem cells 2016; **34**: 2501–2511.
36. C. Y. Lo, et al. Cell surface glycoengineering improves selectin-mediated adhesion of mesenchymal stem cells (MSCs) and cardiosphere-derived cells: Pilot validation in porcine ischemia-reperfusion model. Biomaterials 2016; **74**: 19–30.
37. V. F. Rymsha, et al. Certain clinical and biochemical indicators in chronic pyelonephritis of the solitary kidney. Vrachebnoe delo 1974; **10**: 90–92.
38. T. Isaji, et al. Introduction of bisecting GlcNAc into integrin alpha5beta1 reduces ligand binding and down-regulates cell adhesion and cell migration. J Biol Chem 2004; **279**: 19747–19754.
39. T. Kitada, et al. The addition of bisecting N-acetylglucosamine residues to E-cadherin down-regulates the tyrosine phosphorylation of beta-catenin. J Biol Chem 2001; **276**: 475–480.
40. Y. Kizuka, et al. An aberrant sugar modification of BACE1 blocks its lysosomal targeting in Alzheimer's disease. EMBO molecular medicine 2015; **7**: 175–89.
41. A. Bronisz, et al. Reprogramming of the tumour microenvironment by stromal PTEN-regulated miR-320. Nature cell biology 2011; **14**: 159–167.
42. J. M. Lehmann, G. Riethmüller & J. P. Johnson MUC18, a marker of tumor progression in human melanoma, shows sequence similarity to the neural cell adhesion molecules of the immunoglobulin superfamily. Proc Natl Acad Sci U S A 1989; **86**: 9891–9895.
43. Z. Wang, et al. CD146, from a melanoma cell adhesion molecule to a signaling receptor. Signal Transduct Target Ther. 2020; **5**: 148.
44. M. Trzpis, P. M. McLaughlin, L. M. de Leij & M. C. Harmsen Epithelial cell adhesion molecule: more than a carcinoma marker and adhesion molecule. Am J Pathol 2007; **171**: 386–395.

45. J. Chen, et al. SOX18 promotes gastric cancer metastasis through transactivating MCAM and CCL7. Oncogene 2020; **39**: 5536–5552.
46. L. Harkness, W. Zaher, N. Ditzel, A. Isa & M. Kassem. CD146/MCAM defines functionality of human bone marrow stromal stem cell populations. Stem Cell Res Ther 2016; **7**: 4.
47. S. Stopp, et al. Expression of the melanoma cell adhesion molecule in human mesenchymal stromal cells regulates proliferation, differentiation, and maintenance of hematopoietic stem and progenitor cells. Haematologica 2013:**98**; 505–513.
48. B. Sacchetti, et al. Self-renewing osteoprogenitors in bone marrow sinusoids can organize a hematopoietic microenvironment. Cell 2007;**131**: 324–336.
49. L. B. Li, et al. The role of N-glycosylation in function and surface trafficking of the human dopamine transporter. J Biol Chem 2004; **279**: 21012–21020.
50. P. Wujek, E. Kida, M. Walus, K. E. Wisniewski & A. A. Golabek N-glycosylation is crucial for folding, trafficking, and stability of human tripeptidyl-peptidase I. J Biol Chem 2004; **279**: 12827–12839.
51. Y. Haga, K. Ishii & T. Suzuki. N-glycosylation is critical for the stability and intracellular trafficking of glucose transporter GLUT4. J Biol Chem 2011; **286**: 31320–31327.
52. L. Guzman-Rojas, et al. Cooperative effects of aminopeptidase N (CD13) expressed by nonmalignant and cancer cells within the tumor microenvironment. Proc Natl Acad Sci U S A 2012; **109**: 1637–1642.
53. R. A. Ashmun & A. T. Look Metalloprotease activity of CD13/aminopeptidase N on the surface of human myeloid cells. Blood 1990; **75**: 462–469.
54. M. Ghosh, T. Kelava, I. V. Madunic, I. Kalajzic & L. H. Shapiro CD13 is a critical regulator of cell-cell fusion in osteoclastogenesis. Scientific reports 2021; **11**:10736.
55. I. Ranogajec, J. Jakić-Razumović, V. Puzović & J. Gabrilovac. Prognostic value of matrix metalloproteinase-2 (MMP-2), matrix metalloproteinase-9 (MMP-9) and aminopeptidase N/CD13 in breast cancer patients. Medical oncology 2012; **29**: 561–569.
56. E. Dondossola, et al. CD13-positive bone marrow-derived myeloid cells promote angiogenesis, tumor growth, and metastasis. Proc Natl Acad Sci U S A. 2013; **110**: 20717–20722.

Figures

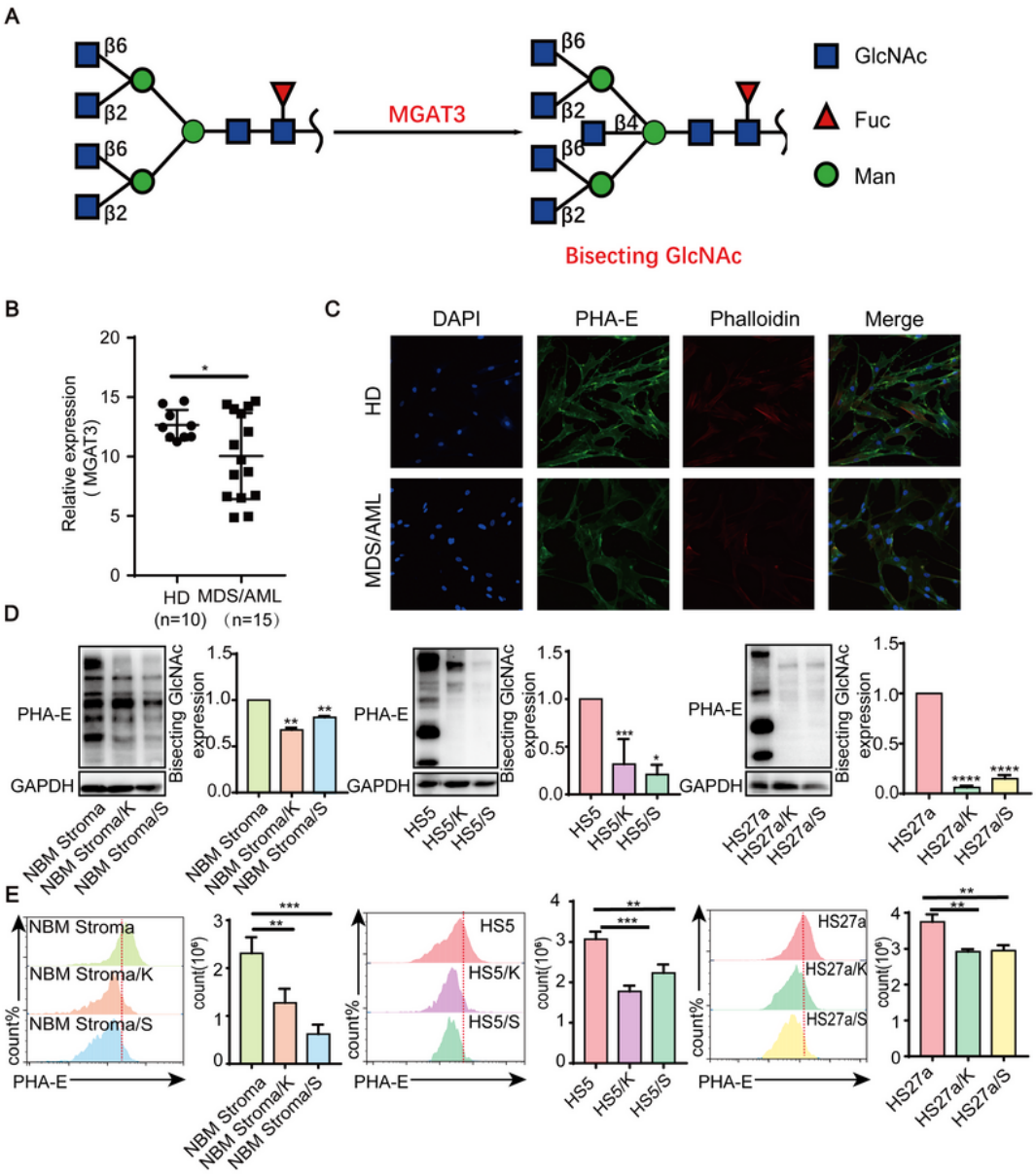

Figure 1

Expression of bisecting GlcNAc in BM stromal cells

(**A**) Typical bisecting GlcNAc structures. (**B**) MGAT3 expression at mRNA level in BM stromal cells from MDS or AML patients. (**C**) Representative confocal microscopic images of MGAT3 and bisecting GlcNAc in BM stroma from healthy subjects and MDS or AML patients. **(D)** Lectin blotting analysis of

bisecting GlcNAc levels in NBM stroma, and in HS5 and HS27a co-cultured with KG1a ("K") or SKM-1 ("S"). Band intensities were quantified using Image J software program. (**E**) FACS analysis of bisecting GlcNAc levels in NBM stroma, and in HS5 and HS27a co-cultured with KG1a or SKM-1. Data were analyzed and quantified using FlowJo software program.

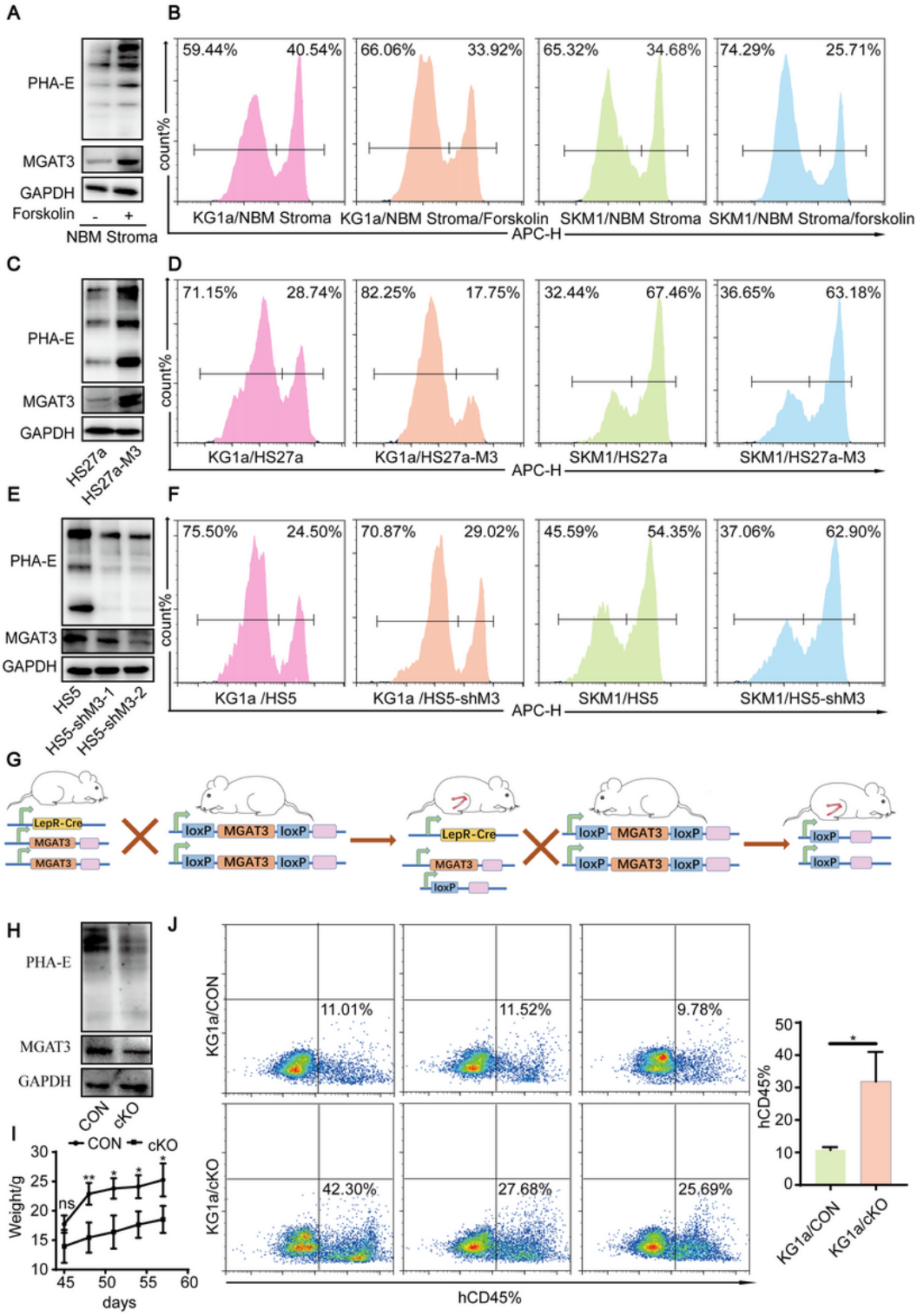

Figure 2

Bisecting GlcNAc in NBM stroma affects myeloid cell proliferation

(**A**) NBM stromal cells were treated with 10 μM forskolin for 12 h, and expression of MGAT3 and bisecting GlcNAc were evaluated by western or lectin blotting. (**B**) KG1a and SKM-1 cells were co-cultured with forskolin-treated or nontreated NBM stroma for 48 h, and their proliferation was assayed by FACS. (**C**) Expression of MGAT3 and bisecting GlcNAc in HS27a and HS27a-M3. (**D**) Proliferation of KG1a and SKM-1 co-cultured with HS27a or HS27a-M3. (**E**) Expression of MGAT3 and bisecting GlcNAc in HS5 and HS5-shM3. **(F)** Proliferation of KG1a and SKM-1 co-cultured with HS5 and HS5-shM3. (**G**) Construction of MGAT3 conditional knockout (cKO) mice (schematic). **(H)** Expression of MGAT3 and bisecting GlcNAc in BM stromal cells derived from *MGAT3*$^{fl/fl}$ and *LepR-cre; MGAT3*$^{fl/fl}$ mice. (**I**) Weights of these mice as a function of time. (**J**) FACS analysis of percentage of KG1a in peripheral blood of these mice.

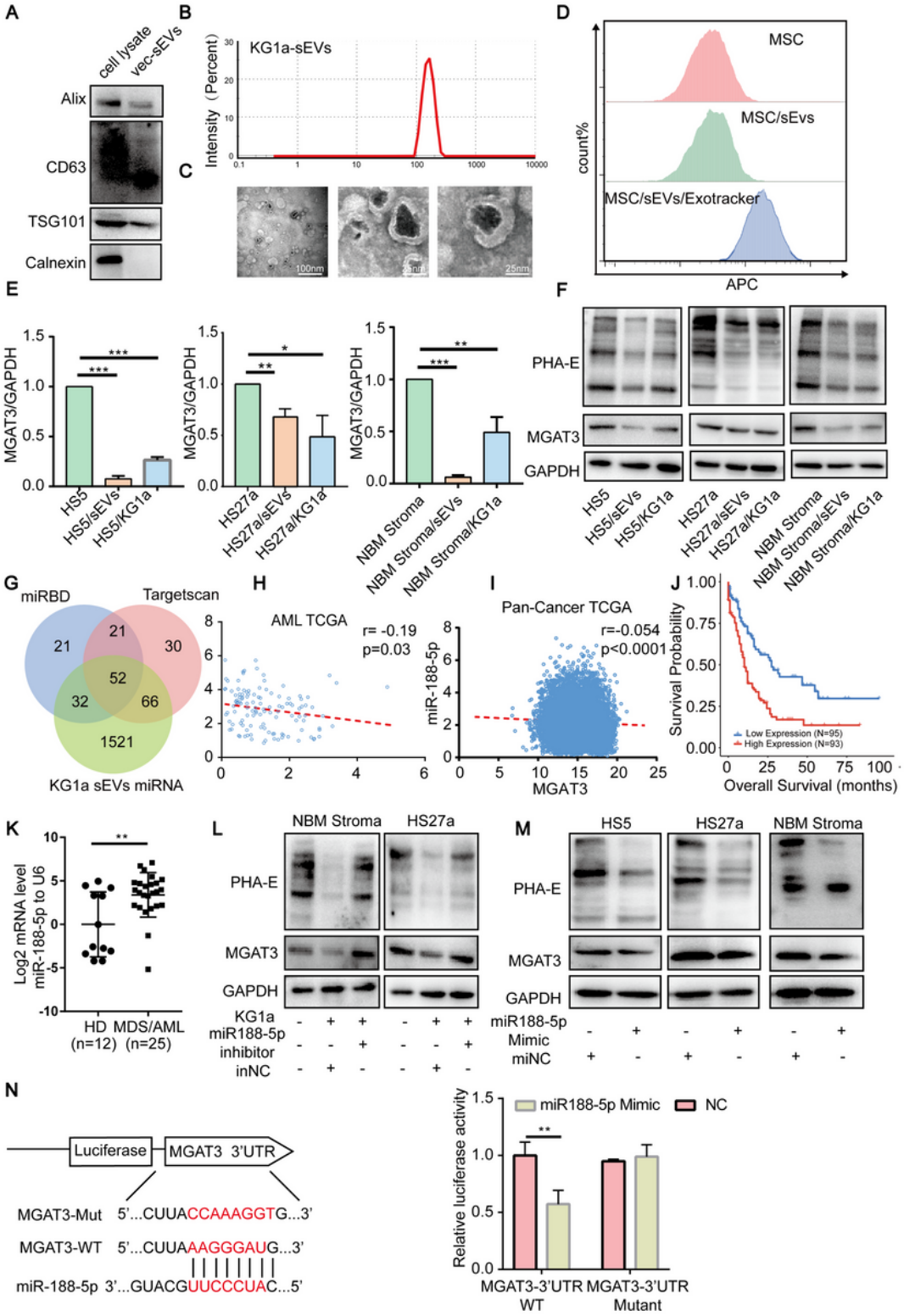

Figure 3

Exosomal miR188-5p inhibits bisecting GlcNAc by targeting MGAT3

(A) Western blotting analysis of exosome marker expression. **(B)** Particle size of KG1a cell exosomes analyzed by nanoparticle tracking analysis (NTA). **(C)** Exosome morphology evaluated by TEM. **(D)** FACS analysis of uptake of ExoTracker-labeled KG1a cell exosomes in NBM stroma. **(E)** MGAT3

expression at mRNA level in HS5, HS27a, and NBM stroma treated with 50 μg/ml KG1a cell exosomes or co-cultured with KG1a. **(F)** MGAT3 expression and bisecting GlcNAc level in HS5, HS27a, and NBM stroma treated with 50 μg/ml KG1a cell exosomes or co-cultured with KG1a. **(G)** Venn diagram of MGAT3 targeted microRNA predicted by TargetScan, miRBD, and miRNA-Seq analysis of KG1a cell exosomes. **(H)** Correlation of MGAT3 and miR-188-5p in AML from TCGA database. **(I)** Correlation of MGAT3 and miR-188-5p in Pan-Cancer, from TCGA database. **(J)** Overall survival of miR188-5p expression in AML patients, from TCGA database. **(K)** miR-188-5p expression at mRNA level in exosomes from plasma of MDS or AML patients. **(L)** NBM stroma or HS27a were co-cultured with miR188-5p inhibitor-treated or miR188-5p inhibitor negative control ("inNC")-treated KG1a cells for 72 h, and bisecting GlcNAc levels were determined by lectin blotting. **(M)** Lectin blotting analysis of MGAT3 and bisecting GlcNAc levels of HS5, HS27a, and NBM stroma treated with miR188-5p mimic. **(N)** HEK293T cells were co-transfected with miR188-5p mimic or miR188-5p mimics negative control ("miNC") and two reporter plasmids psiCHECK2 (wild-type or mutant MGAT3 3'-UTR sequence), and luciferase activities of transfectant cells were assayed.

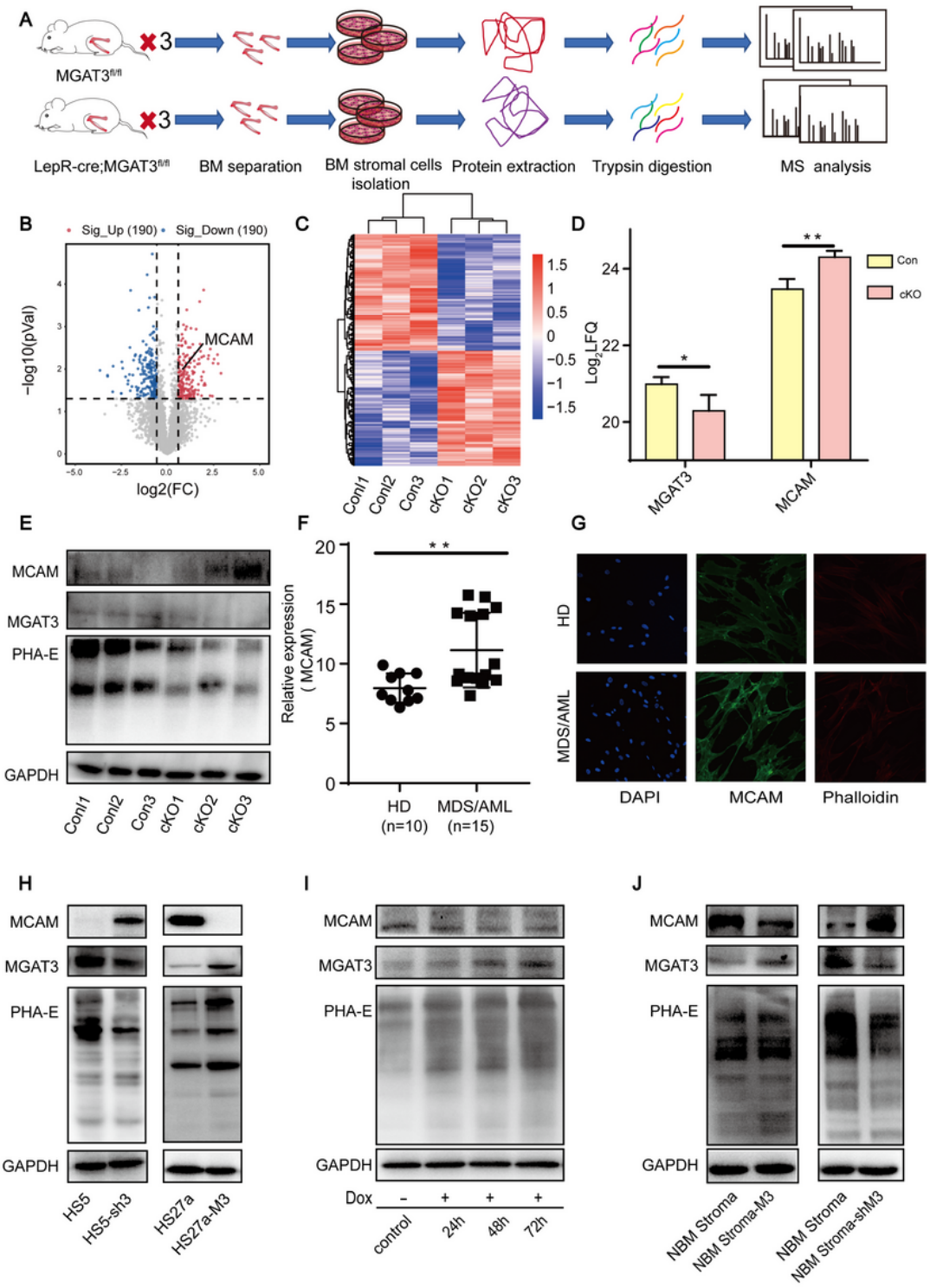

Figure 4

Effect of bisecting GlcNAc on MCAM expression

(**A**) Extraction of BM stromal cells from mouse BM, and MS analysis (schematic). (**B**) Volcano plot of identified proteins in BM stromal cells. log10 p-value is plotted against log2 value (derived from *MGAT3*$^{fl/fl}$ vs. *LepR-cre; MGAT3*$^{fl/fl}$ mice). (**C**) Heatmap of differentially expressed proteins in BM stromal

cells derived from *MGAT3*$^{fl/fl}$ *or LepR-cre; MGAT3*$^{fl/fl}$ mice. Red: upregulation. Blue: downregulation. (**D**) LC-MS analysis of MCAM and MGAT3 expression. (**E**) Expression of MGAT3, bisecting GlcNAc, and MCAM in BM stromal cells from *MGAT3*$^{fl/fl}$ and *LepR-cre; MGAT3*$^{fl/fl}$ mice. (**F**) MCAM expression at mRNA level in BM stromal cells from MDS or AML patients. (**G**) Representative confocal microscopic images of MCAM in BM from healthy subjects and MDS or AML patients. (**H**) Western blotting analysis of MCAM expression in HS27a-MGAT3 and HS5-shMGAT3. (**I**) HS27a-TetOne-MGAT3 cells were treated with 2 μg/ml doxycycline, and expression of bisecting GlcNAc, MCAM, and MGAT3 was analyzed by lectin or western blotting. (**J**) Expression of bisecting GlcNAc, MCAM, and MGAT3 in NBM stroma-MGAT3 and NBM stroma-shMGAT3.

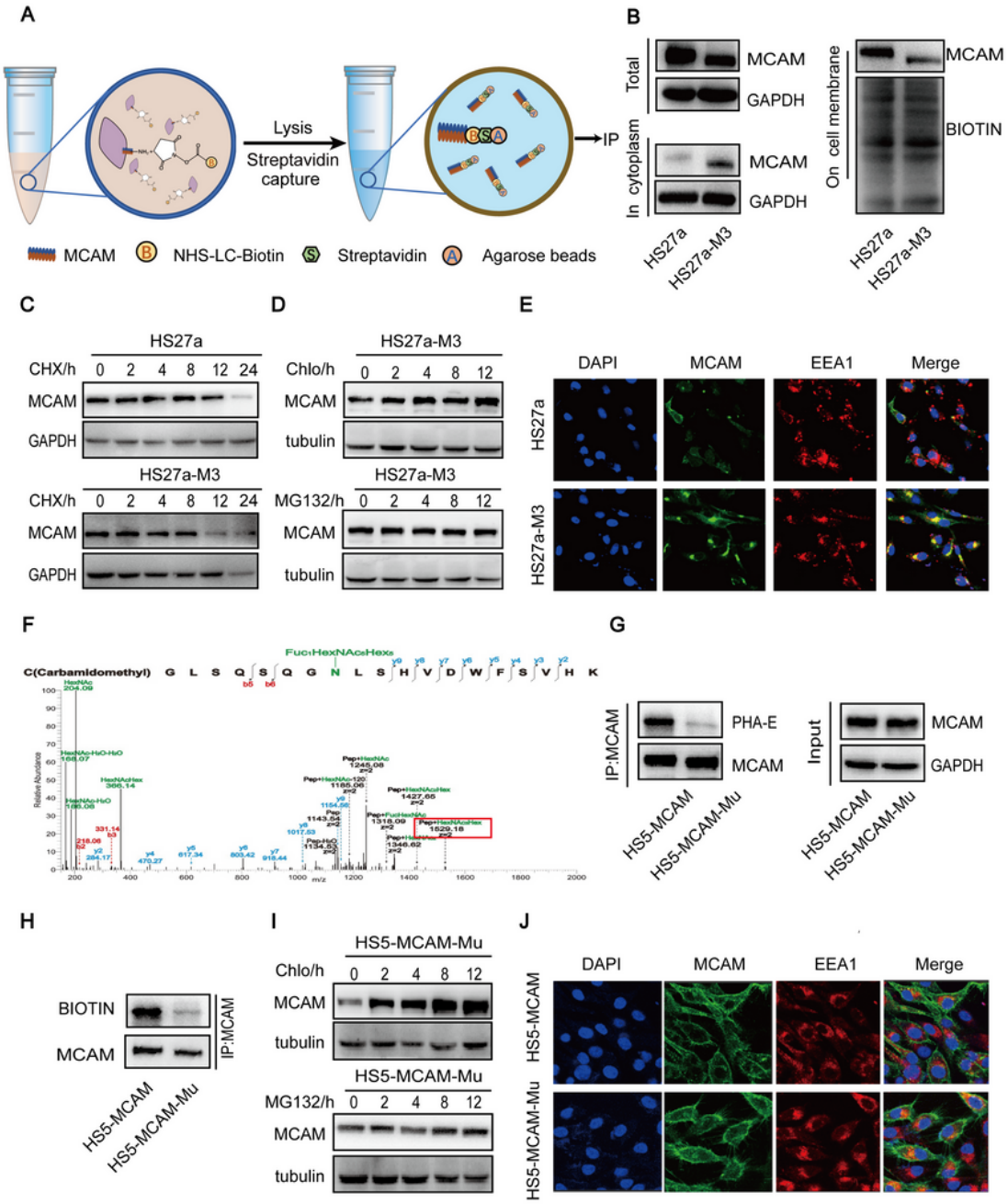

Figure 5

Function of bisecting GlcNAc modification on MCAM

(A) Sulfo-NHS-LC-Biotin labeling of MCAM on cell membrane (schematic). **(B)** Sulfo-NHS-LC-Biotin-labeled MCAM was IP'd by streptavidin-conjugated agarose. Total MCAM in cytoplasm and cell membrane was assayed by western blotting. **(C)** HS27a and HS27a-MGAT3 were treated with

cycloheximide (CHX) for indicated times, and MCAM half-life was evaluated by western blotting. **(D)** HS27a-MGAT3 were treated with chloroquine (Chlo) or MG132 for indicated times, and MCAM expression was assayed by western blotting. **(E)** Confocal microscopic images of MCAM localization in HS27a-MGAT3 lysosomes. EEA1: early endosome antigen 1. **(F)** Representative MS/MS spectra of peptides with bisecting GlcNAc of MCAM in HS5-MCAM. **(G)** Wild-type and mutant MCAM at Asn 56 were overexpressed in HS5, and bisecting GlcNAc on MCAM in HS5-MCAM and HS5-MCAM-Mu was assayed by IP and western blotting. (**H**) IP and western blotting assay of MCAM expression on HS5-MCAM and HS5-MCAM-Mu cell membranes. **(I)** HS5-MCAM-Mu were treated with Chlo or MG132 for indicated times, and MCAM expression was evaluated by western blotting. **(J)** Confocal microscopic images of MCAM localization in HS5-MCAM-Mu lysosomes.

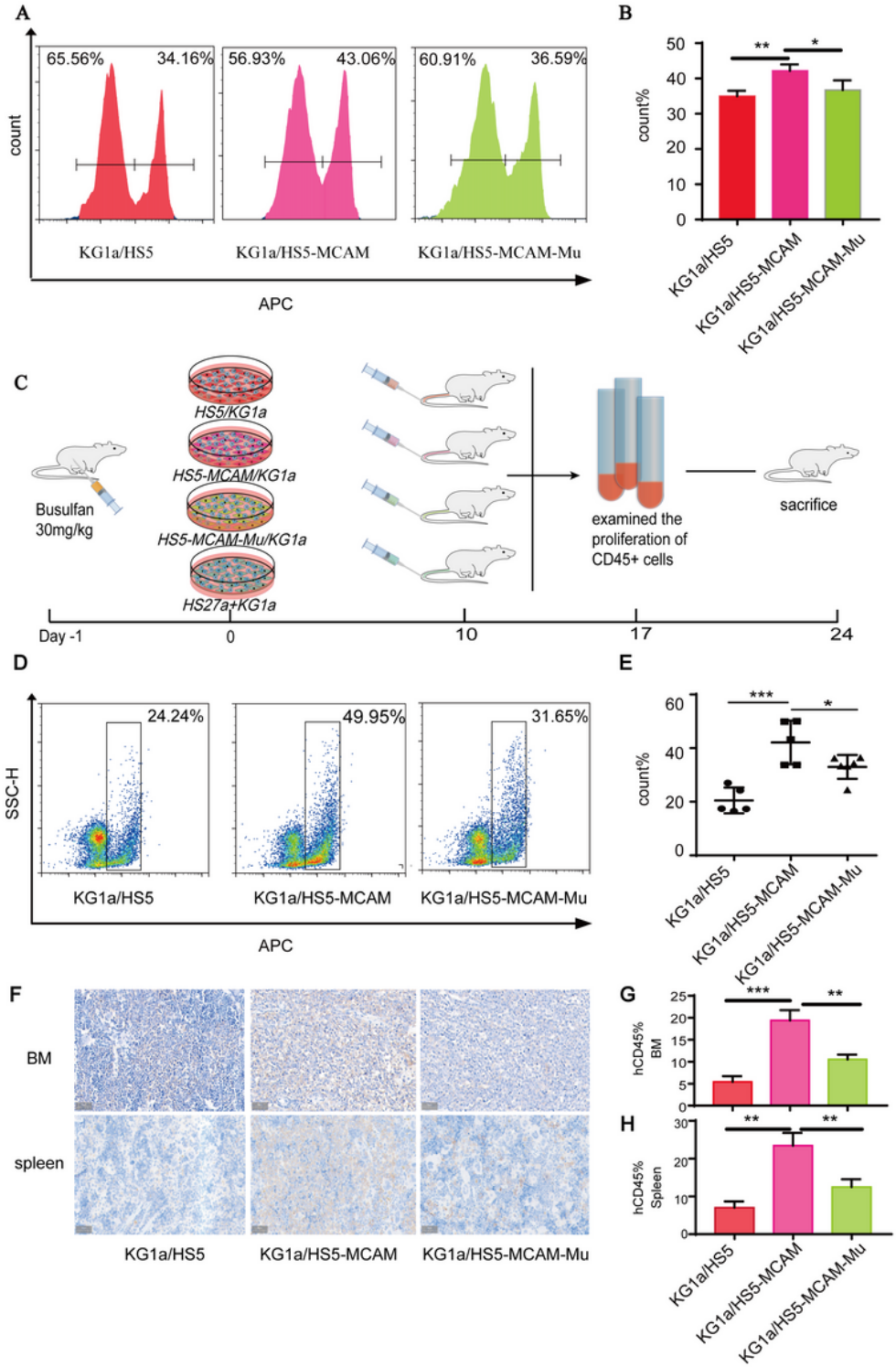

Figure 6

Effect of bisecting GlcNAc modification of MCAM on myeloid cell proliferation

(A, B) Proliferation of KG1a co-cultured with HS5, HS5-MCAM, and HS5-MCAM-Mu. **(C)** *In vivo* mouse model (schematic). NSG mice were treated with 30 mg/kg busulfan for 24 h, injected with mixtures of HS5/KG1a, HS5-MCAM/KG1a, or HS5-MCAM-Mu/KG1a, and peripheral blood was collected

on days 10 and 17. **(D, E)** FACS analysis of KG1a percentages in peripheral blood of NSG mice co-injected with HS5, HS5-MCAM, or HS5-MCAM-Mu. **(F, G, H)** Immunohistochemical staining of CD45 in BM and spleen of NSG mice as above.

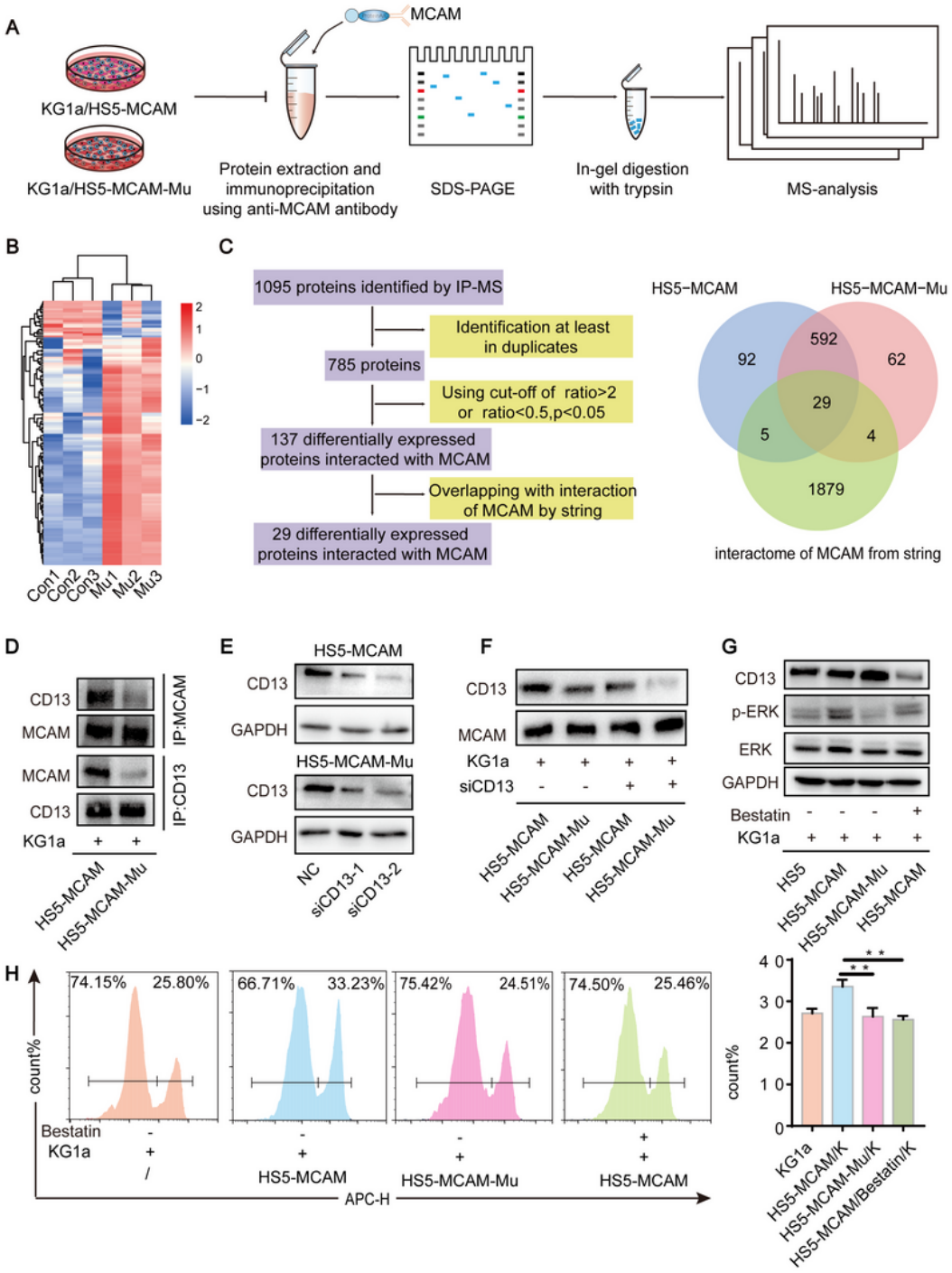

Figure 7

Interaction of KG1a membrane proteins with stromal cell MCAM

(A) IP-MS analysis (schematic). Lysates of stromal cells and KG1a cells were mixed overnight and IP'd with anti-MCAM antibody, and enriched proteins were analyzed by MS. **(B)** Interaction of differentially expressed proteins in KG1a with wild-type or mutant MCAM of HS5-MCAM or HS5-MCAM-Mu was analyzed by IP-MS, and presented as heatmap. Red: upregulation. Blue: downregulation. **(C)** Proteomic analysis of membrane protein interaction with MCAM on KG1a. **(D)** KG1a cells were co-cultured with HS5-MCAM cells or HS5-MCAM-Mu cells overnight. The co-cultured cells were lysed and IP'd with anti-MCAM antibody or anti-CD13 antibody. MCAM/ CD13 interaction were analyzed by western blotting. **(E)** CD13 expression in HS5-MCAM or HS5-MCAM-Mu transiently transfected with CD13 siRNA. **(F)** IP/ western blotting analysis of MCAM/ CD13 interaction in KG1a and CD13 silenced HS5-MCAM or HS5-MCAM-Mu cells. **(G)** Western blotting analysis of CD13, ERK, and P-ERK expression in KG1a pretreated with bestain and co-cultured with HS5, HS5-MCAM or HS5-MCAM-Mu. **(H)** KG1a were pretreated with 20 μM bestatin for 12 h, co-cultured with HS5-MCAM or HS5-MCAM-Mu for 48 h, and cell proliferation was assayed by FACS.

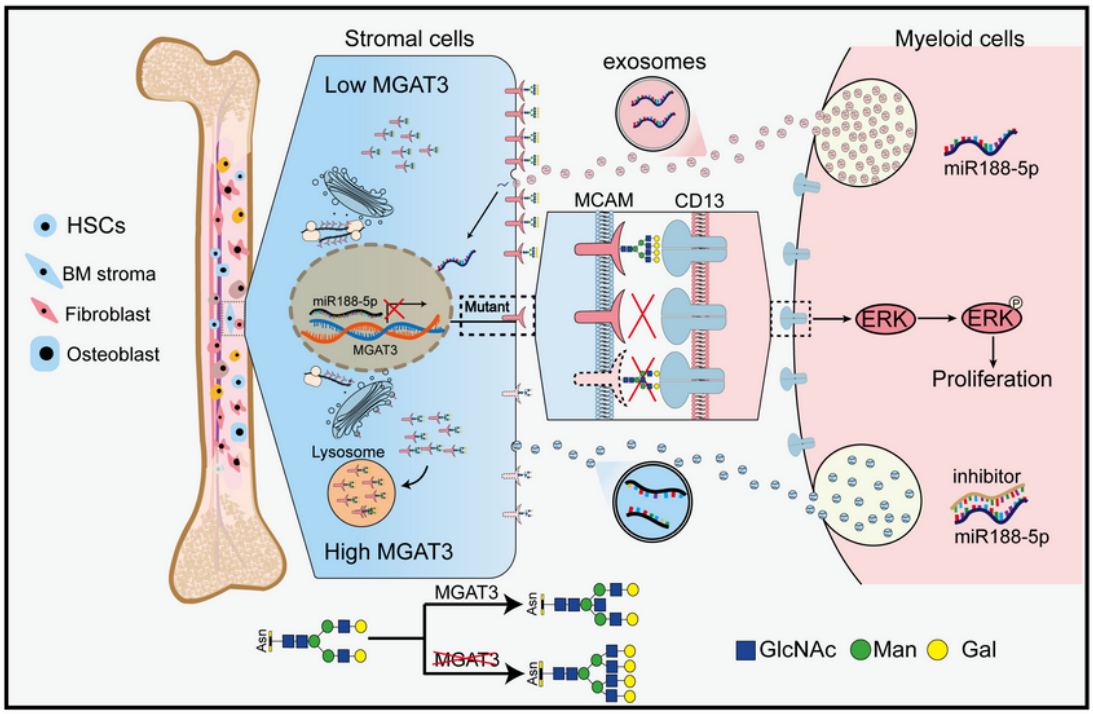

Figure 8

Bisecting GlcNAc on MCAM of BM stromal cells generates a pro-tumoral niche by exosomal miR-188-5p in malignant clonal cells (conceptual model).

Supplementary Files

This is a list of supplementary files associated with this preprint. Click to download.

- IPMSdata.xlsx
- MSdata.xlsx
- RNASeq.xlsx
- supplementaryinformation.docx